# Journal Pre-proof

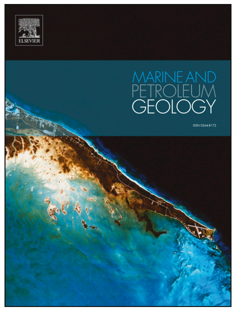


Seal characterization and integrity in uplifted basins: Insights from the northern Barents Shelf

Renate Strugstad Paulsen, Thomas Birchall, Kim Senger, Sten-Andreas Grundvåg

PII: S0264-8172(22)00066-6

DOI: https://doi.org/10.1016/j.marpetgeo.2022.105588

Reference: JMPG 105588

To appear in: *Marine and Petroleum Geology*

Received Date: 22 February 2021

Revised Date: 10 February 2022

Accepted Date: 12 February 2022

Please cite this article as: Paulsen, R.S., Birchall, T., Senger, K., Grundvåg, S.-A., Seal characterization and integrity in uplifted basins: Insights from the northern Barents Shelf, *Marine and Petroleum Geology* (2022), doi: https://doi.org/10.1016/j.marpetgeo.2022.105588.

# Seal Characterization and Integrity in Uplifted Basins: Insights from the northern Barents Shelf

**Renate Strugstad Paulsen[1], Thomas Birchall[2], Kim Senger[2], Sten-Andreas Grundvåg[1]**

[1]Department of Geosciences, UiT - The Arctic University of Norway, Tromsø, Norway

[2]Department of Arctic Geology, The University Centre in Svalbard, Longyearbyen, Norway

Renate.S.Paulsen@uit.no

**Abstract**

**Seal integrity is a key property for petroleum exploration. This is even more the case in uplifted basins, as exemplified by the northern Barents Shelf. Uplift may lead to fracturing, decompaction, gas expansion and fluid flow. Therefore, it is critical to understand the mechanical behaviour of the Jurassic shale caprocks in the Greater Hoop area, where hydrocarbon accumulations are situated as little as 250 m below the seabed. In this contribution we study the Upper Jurassic Fuglen and Hekkingen formations. We analyse the mechanical properties of six wells in the study area in combination with leak-off tests and 3D seismic data to characterise the caprock variability over the area. Ductility appears to be largely a response to total organic content, with overall sealing properties appearing exceptionally good in southern parts but diminishing to the north in the study area due to increasing silt content and thinning of the more organic rich Hekkingen Formation.**

Key Words: Cap Rock, Shales, Rock physics, Burial and uplift, Hoop Fault Complex, Exhumation

## 1. Introduction

The Barents Sea represents the northernmost province for hydrocarbon exploration on the Norwegian Continental Shelf (NCS) (Fig 1). Exploration success has to date been limited, with only two producing fields: the Snøhvit and Goliat fields) and several discoveries in the development phase. The Wisting discovery is one such example, situated 250 m below the seabed in the uplifted northern Barents shelf. Uplift provides an additional risk to seal integrity so developing a better understanding of shale behaviour during and after uplift is critical for this part of the continental shelf.

Uplift and erosion are typically associated with the deterioration of seal integrity. Thus, sedimentary basins which have undergone severe uplift are commonly considered high-risk exploration targets. In general, sediments undergo embrittlement during deep burial, as the mechanical and chemical change due to increasing temperature and pressure. The shale-dominated, Upper Jurassic – Lower Cretaceous Hekkingen Formation is one of the most important cap rock units of the Barents Shelf and provides the top seal for both producing fields and all the discoveries in the study area. It is also widely regarded as an immature source rock throughout the northern parts of the Barents Shelf, although total organic carbon (TOC) values typically ranging between 5–15%. The underlying Upper Jurassic Fuglen Formation is also shale-dominated, but generally exhibits lower TOC content compared to the Hekkingen Formation. Collectively, these units form a regionally important cap rock succession (Ronnevik et al., 1982, Gabrielsen and Kløvjan, 1997, Nooraiepour et al., 2017), but they also represent important source rocks in other parts of the Barents Shelf (Henriksen et al., 2011, Løseth et al., 2011, Duran et al., 2013, Abay et al., 2018, Koevoets et al., 2018a).

Fundamentally, for leakage to occur there must be a driver for fluid flow and the seal must be overcome through mechanical or capillary processes. Uplift can cause changes in seal properties and in the PVT conditions of subsurface fluids to initiate such leakage. In most sedimentary basins of the world, overpressure is a main driver of fluid flow (Bjørlykke, 1993). In our study area, there is no evidence of overpressure (Birchall et al., 2020b), yet there is clear evidence of ongoing migration. This is likely caused by changes in PVT conditions of both the rocks and fluids, with gas exsolution and expansion also playing a role in driving fluid flow.

Brittleness is an important aspect to consider when it comes to characterizing the mechanical properties of rocks, particularly for investigating whether fracture networks may have developed during uplift. The caprocks' ability to retain hydrocarbons after uplift is also strongly influenced by external forcing factors such as regional stress, fault, and lithology. The Barents Shelf has been subject to pronounced glacial loading and unloading throughout recent geological history (Løtveit et al., 2019). Mudrocks with high quartz content may behave in a more brittle way in exhumed basins due to the chemical compaction it experiences during subsidence as discussed by Makurat et al. (1992), and Gabrielsen and Kløvjan (1997) in their study of the Fuglen and Hekkingen formations in the southwestern Barents Sea.

Previous studies from the SW Barents Sea, have suggested that vertical leakage at fault intersections is the main controlling factor for gas-water contacts (Hermanrud et al., 2014a, Edmundson et al., 2020). The underfilling of structures is common in areas that have undergone uplift and following erosion (Doré et al., 2002). Many studies have tried to quantify the amount of uplift and erosion (Henriksen et al., 2011, Baig et al., 2016, Ktenas et al., 2017, Lasabuda et al., 2018) to mention some in order to understand the impact it has on hydrocarbon generation and trapping. Although much work has been focused on the properties of reservoir sandstones on the NCS (Olsen et al., 2017, Bukar et al., 2020) there are few published studies directly related to the understanding of cap rock shales and mudstones during and after uplift. Cap rock shales and mudstones may act differently on the local scale compared to the regional scale due to heterogeneity resulting from input of coarser grained sediment during deposition (Perez Altamar and Marfurt, 2015).

Here, we investigate the mechanical properties and regional distribution of the Upper Jurassic – Lower Cretaceous shales of the Fuglen and Hekkingen formations in and around the Hoop Fault Complex (HFC) on the northern Barents Shelf. Based on extrapolation of petrophysical data from well-logs (Fig. 3) we calculate and correlate elastic properties with depth, density, and velocity data. We also assess the mechanical strength of the caprock using leak-off test (LOT) and extended leak-off test (XLOT) data. Further, we link the investigated wells to 3D seismic data to investigate the thickness, extent, and physical properties of the Fuglen and Hekkingen Formations in our study area (Fig. 1).

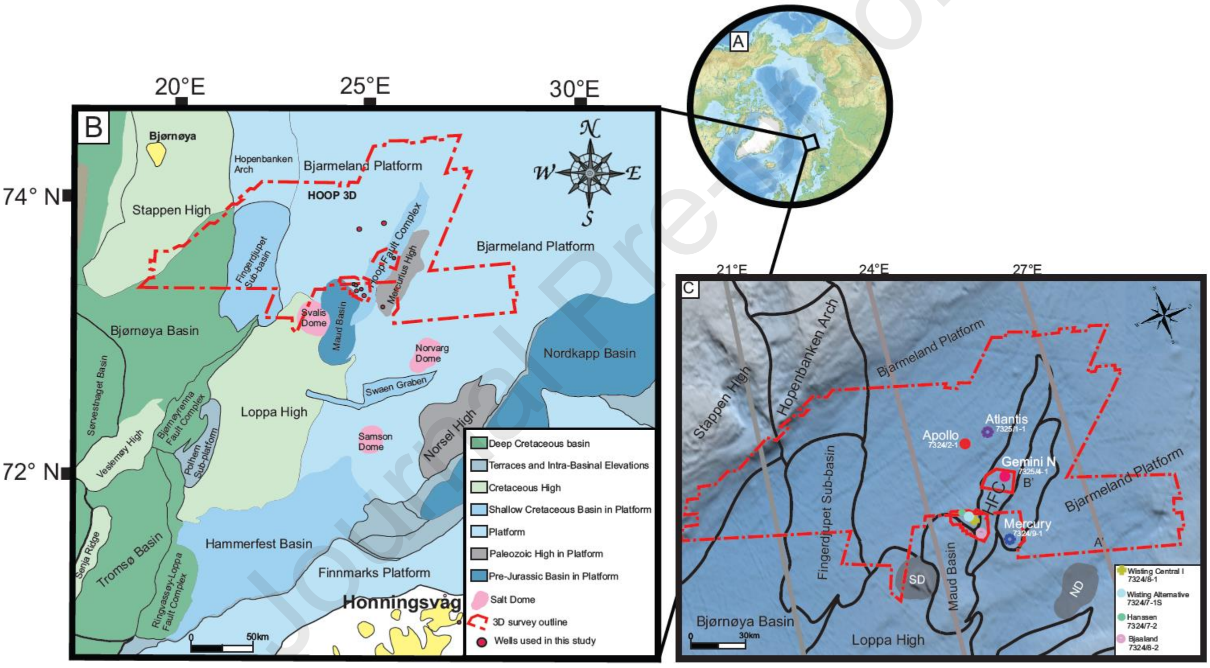


**Figure 1** (a) Location of the Barents Shelf. Bathymetry map from (B) Map showing the outline of the study area and nearby structural elements including outline of 3D Seismic surveys and well positions (C) Detailed location map of the wells and seismic surveys investigated in this study and seabed bathymetry adapted after Jakobsson et al. (2012). The structural elements in (B) and (C) are adapted from NPD (NPD, 2020). SD: Samson Dome, ND: Norvarg Dome.

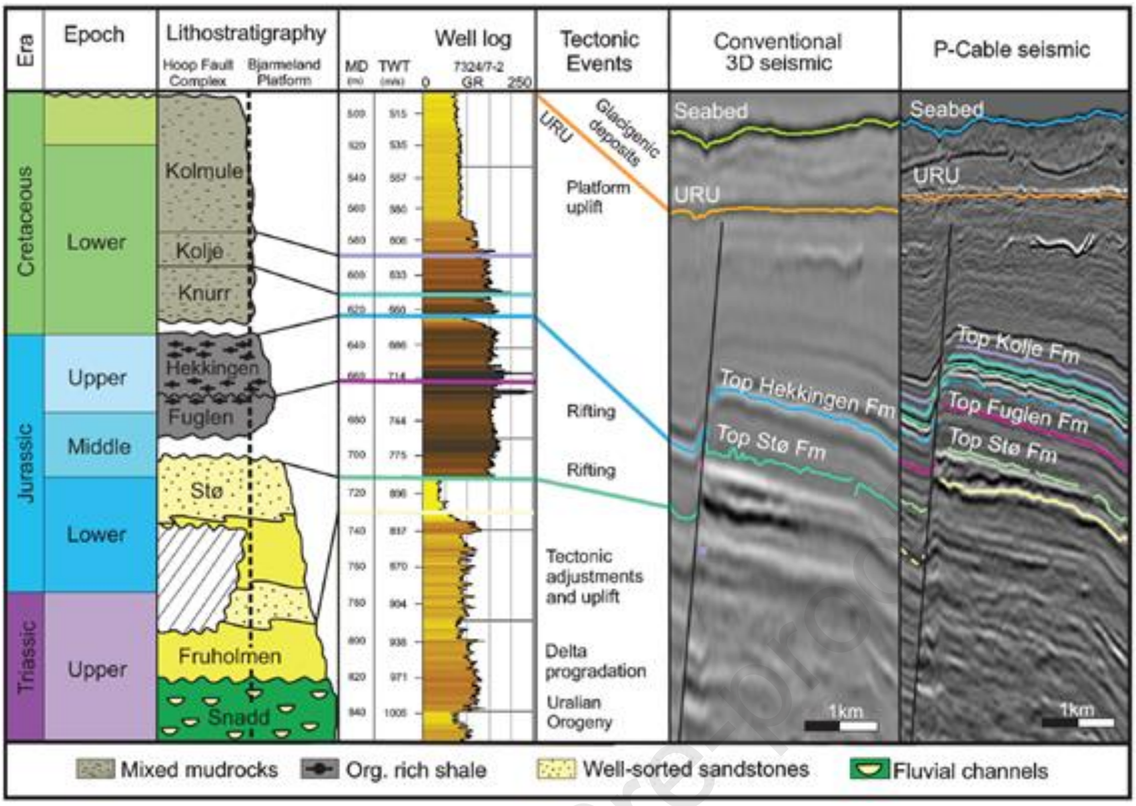


**Figure 2** Conceptual chronostratigraphic chart of the Mesozoic succession in the HFC and Bjarmeland Platform (adapted after NPD) correlated to well log data (gamma ray-response from well 7324/7-2). This study investigates mudrocks of the Upper Jurassic to Lower Cretaceous Fuglen and Hekkingen formations. The underlying Stø Formation represents the most important reservoir unit on the Barents Shelf. A comparison between conventional 3D seismic and P-Cable seismic is shown to illustrate the difference in seismic resolution between such datasets, further demonstrating the advantage of using high resolution P-Cable seismic in shallow and uplifted areas on the Barents shelf. URU: Upper Regional Unconformity.

## 2. Geological setting

The Hoop area is located in the central parts of the Bjarmeland Platform (Fig. 1). The majority of the basins, highs and fault complexes developed prior to the opening of the NE Atlantic in the Early Cenozoic (Faleide et al., 1993a, Smelror et al., 2009). Multiple episodes of rifting and subsequent subsidence have laid the foundation for the present-day structural framework (Gabrielsen et al., 1990b, Doré, 1995, Faleide et al., 2008, Henriksen et al., 2011a). During the progressive northward opening of the Central Atlantic in the Mesozoic to early Cenozoic many of these inherited structures underwent reactivation (Faleide et al., 2008). The HFC is an example of this and is recognized by its deep-seated faults that are cutting through the Carboniferous stratigraphy (Gabrielsen et al., 2016, Collanega et al., 2017). These deep-seated faults are overlain by a younger faulted succession of Triassic and Jurassic age. The younger faults are off-setting the Triassic, Jurassic and Cretaceous sediment packages and thus form some of the most important fault-bounded closures in the area including the Wisting and Hanssen discoveries. Repeated episodes of tectonic movement have also led to remobilization of salt, which in the Triassic led to the formation of the Maud Basin that constrains the south distribution of the HFC (Gabrielsen et al., 2016). Throughout the Triassic – Middle Jurassic, the Barents Shelf developed into a shallow marine environment with prevailing deposition of sand on the platform (Glørstad-Clark et al., 2010). During the major rift phase in the Late Jurassic and Early Cretaceous, mud-rich successions were deposited under a regional transgression (Serck et al., 2017a, Marín et al., 2020). The rift topography in combination with the relative rise in sea-level promoted the development of restricted bottom circulation and anoxic conditions that were ideal for the preservation of organic material. The resulting mud-dominated deposits represent basin-wide shale-rich units with elevated TOC contents, which make ideal top seal candidates and regional source rock units (Riis and Halland, 2014).

### 2.1 The Greater Hoop area

Our study area is situated on the central parts of the Bjarmeland Platform on the eastern side of the Loppa High and includes structural elements such as the Hoop Fault Complex (HFC), the Maud Basin and the Mercurius High. The area is constrained by the Fingerdjupet Sub-basin (FSB) to the west, and to the south by the Loppa High, Svalis Dome and Maud Basin (Fig. 1). To the east, it extends across the Mercurius High and across the western part of the Bjarmeland Platform. The general estimates of net erosion around the HFC are between 1400 m – 2000 m (Amantov et al., 2011, Baig et al., 2016, Henriksen et al., 2011b, Lasabuda et al., 2018).The Hekkingen Formation is immature in the study area and although there is no directTOC data in the study area, data from the Mjølnir Impact crater some 120 km east of the Hoop area indicates a TOC of between 17–34 % in the lower parts of the formation (Dypvik et al., 2010). Other studies from the SW Barents Sea (Ohm et al., 2008a). show an average for upper Hekkingen at 10% TOC and close to 3% for the lower parts. Additionally, data from the Agardhfjellet Formation in Svalbard, the onshore equivalent to the Hekkingen Formation have measured TOC values in the range of 3-16% .

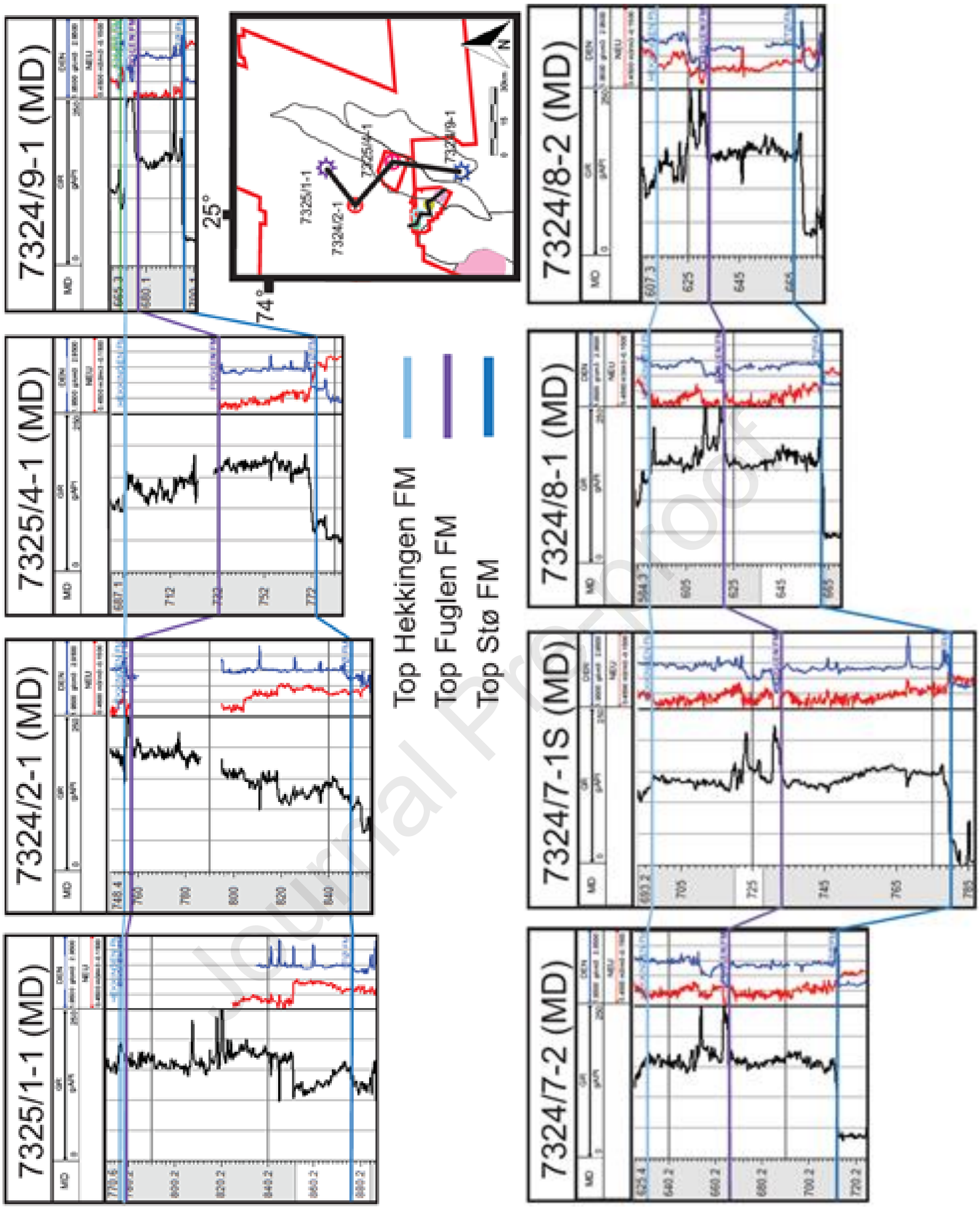


**Figure 3** Well-correlation chart (well locations and distance between each well is shown in Fig. 1 A, B and in inset map in the middle). The correlation panel has been flattened at the top of the Hekkingen Formation. The well tops are correlated according to their wireline readings and available biostratigraphy data from well 7324/2-1.

## 3. Data and methods

### 3.1 Well data

Our well database comprises publicly available exploration wells and seismic data from the DISKOS database. Wells included are summarized in Table 2. Most wells have standard petrophysical logs included. Atlantis (7325/1-1), Apollo (7324/2-1), Gemini Nord (7325/4-1), Wisting Central I (7324/8-1), and Bjaaland (7324/8-2) did not have complete neutron and density logs readings within the Fuglen and Hekkingen formations, and therefore contribute fewer data points to the crossplots. Apollo (7324/2-1), Atlantis (7325/1-1) and Hanssen (7324/7-2) needed manual velocity adjustment, and for the Apollo (7324/2-1) and Atlantis (7325/1-1) wells, a shared checkshot from the Hanssen (7324/7-2) well was used for velocity adjustments.

### 3.2 DlogR – Passey's method

Passey et al,. (1990) developed a method for estimating and calculating TOC in shales using the overlay of a properly scaled resistivity and sonic travel-time wireline logs. The method isalso known as DlogR, where the DlogR represents the calculated difference between the resistivity and porosity log (Passey et al., 1990). If the curves show good separation, it indicates that the interval is a good source rock. On the contrary if there are longer intervals with overlap, it is called a baseline and should represent an interval of non-source rocks. Before calculating the DlogR, the curves must be scaled relatively to each other so that 50 µsec/ft corresponds to one logarithmic step (Passey et al., 1990).

When combining the acoustic slowness (sonic) and resistivity curves we can use the following equation to calculate DlogR: $DlogR = log_{10} (R/R_{baseline})+0.02 \times (\Delta t/\Delta t_{baseline})$. $R$ is the resistivity readings from the wireline (ohm x m), $R_{baseline}$ is baseline values from overlapping curve-interval. $\Delta t$ is the AC (sonic log/acoustic slowness) readings (µs/ft), and $\Delta t_{baseline}$ is the baseline readings from the overlapping curve-interval. This approach is taken to increase our confidence in the TOC content of the Jurassic shales. Although many other studies from the Barents Sea and analogues from Svalbard point towards a generally high TOC Hekkingen Formation (Ohm et al., 2008a, Dypvik et al., 2010, Hansen et al., 2020) to mention some), the Fuglen Formation often shows a more heterogenous well-log response and is less studied.

### 3.3 Well-log parameter modelling

The in-situ mechanical and elastic properties of the investigated cap rocks can be calculated through log-derived dynamic constants (Perez Altamar and Marfurt, 2015). The elastic constants are defined by the Biot-Gassman theory and are often used for reservoir monitoring, and velocity analysis in unconsolidated and consolidated sediments (Carcione et al., 2000, Lee, 2002a).The Poisson's ratio ($v$) can be derived directly from the shear- and compressional velocities where $v = (0,5(Vs/Vp)^2)-1/((Vs/Vp)^2-1)$ and the Young's modulus (E) depend on the velocities and the density of the rock: $E = \rho * Vs^2(3*Vp^2-4*Vs^2)/(Vp^2-Vs^2)$, where $\rho$ = bulk density (which can be measured with a wireline tool). A cross-plot of the Vp/Vs ratio against the acoustic impedance (AI) or density, which can be a powerful tool for lithology analysis, is used to identify fluid phases in reservoir rocks. The Vp/Vs directly related to the Poisson's ratio and can be expressed as $Vp/Vs = \sqrt{2(1-v)/(1-2v)}$. In cases where only the compressional wave is present, density and shear velocity have been derived from this elastic property to create acoustic and shear impedances. The elastic parameters are related, and therefore a good way to correlate cap rocks on a local and regional scale where well-data is available. We aimed our focus to the elastic parameters of Young’s Modulus and Poisson’s ratio. In general, Young’s modulus is referred to as the modulus of elasticity, and it is a measure of how stiff a solid material is behaving. The greater the value, the more resistant a rock is to deformation. The Poisson’s ratio determines the extent to which compression or tension in one direction produces expansion or contraction perpendicular to the applied force. When plotted against each other, the Poisson’s ratio reflects the rock’s ability to fail under stress, while Young’s Modulus reflects the rock’s ability to maintain fractures (Mathia and Ratcliffe, 2016).

**Table 2** Overview of the exploration wells and discoveries investigated in this study. All wellbores in this table are vertical.

| **Well**<br><br>**Prospect** | **Hydrocarbon Content** | **Thickness Fuglen Fm./Hekkingen Fm (m)** | **Depth to top seal**<br><br>**(m MD)** | **Primary Target** | **Water depth (m)** |
|---|---|---|---|---|---|
| 7324/7-2<br><br>**Hanssen** | Oil/gas | 46/36 | 630 | Realgrunnen Subgroup (Stø, Tubåen and Fruholmen fms.) | 417.5 |
| 7324/8-1<br><br>**Wisting Central** | Oil | 41/31 | 590 | Realgrunnen Subgroup (Stø, Tubåen and Fruholmen fms.) | 398 |
| **7324/7-1S**<br>**Wisting Alternative** | | 47/36 | 697 | Upper Triassic Snadd Fm | 413 |
| 7324/8-2<br>**Bjaaland** | Dry (oil shows) | 32/44 | 613 | Realgrunnen Subgroup (Stø, Tubåen and Fruholmen fms.) | 394 |
| 7324/2-1<br><br>**Apollo** | Dry (oil shows) | 92/2 | 755 | Realgrunnen Subgroup (Stø, Tubåen and Fruholmen fms.) | 444 |
| 7325/1-1<br><br>**Atlantis** | Gas | 97/3 | 776 | Middle Triassic (Kobbe Fm.) | 487 |
| 7324/9-1<br><br>Mercury | Gas | 21/4 | 671 | Realgrunnen Subgroup (Stø, Tubåen and Fruholmen fms.) | 414 |

| | | | | | |
|---|---|---|---|---|---|
| 7325/4-1 | Gas/Oil | 40/40 | 692 | Realgrunnen Subgroup (Stø, Tubåen and Fruholmen fms.) | 447 |
| Gemini N**ord** | | | | | |

### 3.2 Seismic data

Three 3D seismic data sets are provided by TGS and consist of both conventional 3D data and high-resolution shallow P-cable seismic data; all surveys are zero-phase polarity, so a peak (red reflector) corresponds to an increase in acoustic impedance. The main dataset (HOOP 3D) covers most of the western part of the study area (Fig. 1b and c) while TGS16004 and the HR14 are smaller high-resolution 3D seismic datasets covering the Wisting and Gemini Nord wells respectively. Table 1 summarizes the general seismic data and their well-coverage. The vertical resolution is calculated using the formula for vertical seismic resolution $\lambda/4$ where $\lambda = v/f$ and $\lambda$= wavelength, v = velocity and f = frequency. The average velocity of the Upper Jurassic shales in the P-cable datasets ranges from 2000 – 2500 m/s. The seismic data has been used for formation correlation between wells, and as a tool for analysing potential high-risk areas for changes in seal integrity (e.g. amplitude anomalies, seismic horizons, attribute- and fault analysis).

**Table 1** Overview of 3D seismic surveys and well coverage included in the study.

| Survey | Provider | Year | Area coverage ($km^2$) | Vertical resolution* (m) | Frequency range (Hz) | Well coverage |
|---|---|---|---|---|---|---|
| HOOP 3D | TGS | 2016 | 22600 | 20 | 10 - 25 | 7324/2-1,7325/1-1, 7325/4-1 |
| HR14_3D_HFCE1 | TGS | 2016 | 367 | 4-5 | 100-120 | 7325/4-1 |
| TGS16004 | TGS | 2014 | 181 | 5-6 | 80-120 | 7324/8-1, 7324/8-2, 7324/7-1S, 7324/7-2 |

### 3.3 Identification of top seal

The Top Seal/Top Hekkingen Formation is easily identifiable throughout the Barents Shelf and is recognized as a strong negative reflector (blue). The Hekkingen and Fuglen formation thins out laterally northwards. The Hekkingen Formation is well-tied to the seismic data in all wells by use of checkshots in the study area and is recognized by a sharp increase in the gamma ray response in a well (Fig 3). For further QC of the well-tie, the gamma ray has been compared with the sonic log, neutron porosity and resistivity log to improve identification of each zone shown in Fig. 2. Because of the high seismic resolution in the P-cable seismic datasets (down to 4 m in some cases, see Table 1), it is also possible to differentiate the Hekkingen Formation from the Fuglen Formation. This is not possible in the conventional 3D data set of lower resolution (Table 1). The Fuglen Formation is also easily recognized in the wells with its sharp gamma ray transition from the overlying Hekkingen (Fig. 3). Lithology identification is based on the gamma ray, sonic velocity and neutron porosity response in the wells listed in Table 2 in addition to data from NPD (e.g., cuttings and cores). The sampling interval in the wells is 15 cm. There is no XRF or mineralogy data available from the Upper Jurassic interval in the wells we've used for this study; therefore, no exact mineral composition can be presented. However, previous studies have covered the Hekkingen Formation on the Barents Shelf and its onshore time-equivalent formation on Svalbard (Abay et al., 2018, Dypvik et al., 1991, Koevoets et al., 2016a, Nooraiepour et al., 2017) which show similar results and interpretations for the Fuglen and Hekkingen formations.

### 3.4 Leak-off tests

Leak-off tests are carried out during drilling to ascertain the mechanical strength of a formation of interest, generally in order to ascertain what drilling mud density can be used without losing control of the wellbore. Pressure against the formation is increased through increased pumping with the rest of the wellbore cased. Pressure increases until the rock begins to fracture (the fracture pressure) and breakdown. When the pumping is lowered again, the fractures begin to close (the fracture closure pressure), and because fractures open perpendicular to the minimum stress direction it approximately represents the regional minimum stress value. A large difference between the initial leak-off pressure and the fracture closure pressure represents the tensile strength of the rock. Extended leak-off tests repeat the cycles of building up and lowering pressures to improve the accuracy of stress measurements. This is important in the Northern Barents shelf as a fractured caprock may be identified by leak-off pressures being very similar to fracture closure pressures. Formation integrity tests (FITs) are carried out to a predetermined pressure to ensure the formation can withstand the planned drilling fluid but does not aim to break the rock.

## 4. Results

### 4.1 Seismic Interpretation

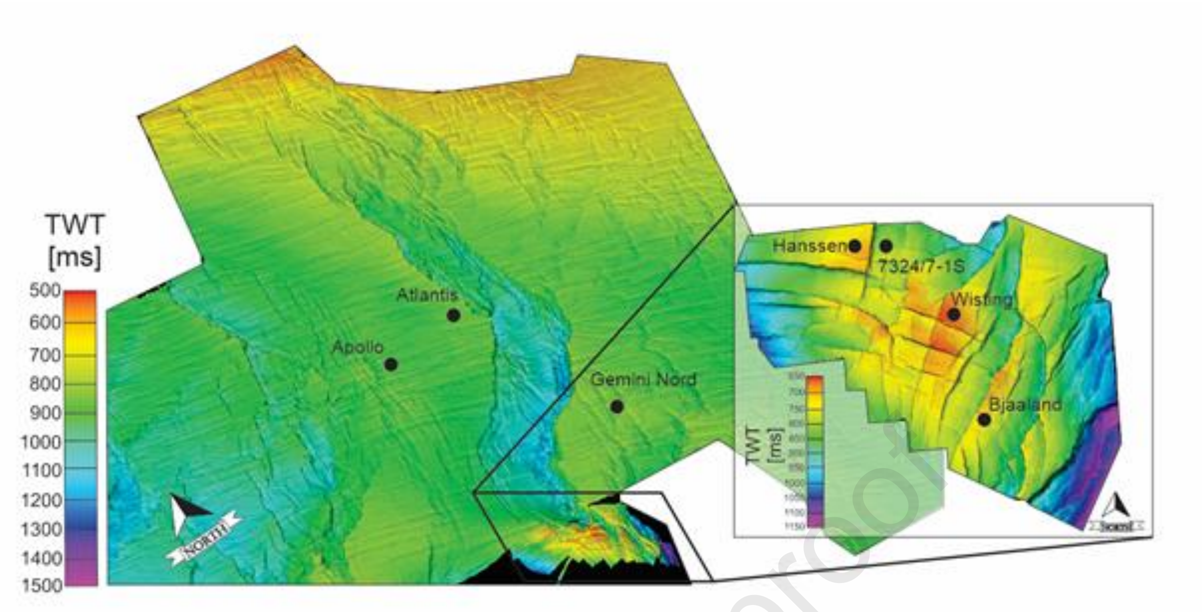


**Figure 4** Seismic TWT map based on the interpretation of the Top Hekkingen reflector from both 3D conventional seismic data (HOOP 3D) and the High-resolution P-cable data TGS16004 from Wisting. Inset map shows a close-up of the Wisting anticline and well locations The blue area west of the Gemini Nord and north of the Wisting show the outline of the Hoop graben, while the Gemini N well is located within the HFC. Apollo and Atlantis are located on the platform area west of the HFC. The location of both seismic surveys is provided in Fig. 1.

The Wisting area represents a four-way closing anticline structure sandwiched between the southern termination of the HFC and the Maud Basin (Fig. 1). The anticline is highly compartmentalized and dominated by NE -SE, NNE-SSW and N-S trending faults crosscutting the Upper Jurassic Fuglen and Hekkingen formations and juxtapositioning the reservoir against the formations in several places (Fig. 5). The overlying Cretaceous sequence is highly eroded on the crest of the anticline and two larger amplitude anomalies are observed from an RMS amplitude extraction in -50 ms window below the URU reflector (Fig. 5 inset map). The Wisting discovery (well 7324/8-1) is oil, we can therefore assume that the gas exsolved during uplift has somehow escaped the reservoir while oil is retained. Exactly why this is the case is not yet fully understood. We observe amplitude anomalies directly above or in relation to underlying Jurassic faults co-sharing the same S-E strike direction. Fig 5 shows close-ups of the fault structures where the Bjaaland well is located (see Fig. 4 for well location) and associated amplitude anomaly (increase in amplitude signal) from two different angles (see inset map in Fig 5 for location of seismic profiles). These anomalies are following the fault trend of the "feeder faults" that are potential migration pathways for these high-amplitude anomalies. We also observe fault-splaying from the upper fault tips of the Jurassic faults that are related to similar amplitude anomalies, in addition to what appear to be polygonal-like faults within the Kolmule strata. The anomaly is widely dispersed above the fault plane indicating diffusive leakage or migration through fault leakage and these "feeder faults". The Bjaaland well was dry with oil shows, and the underlying Stø and Fruholmen formations were water wet, while the Wisting discovery well encountered a 55m oil column 6 km NE of the Bjaaland well within the Stø Formation. However, both wells share the same elastic response expected of a ductile seal (see Fig. 6 and Fig. 8).

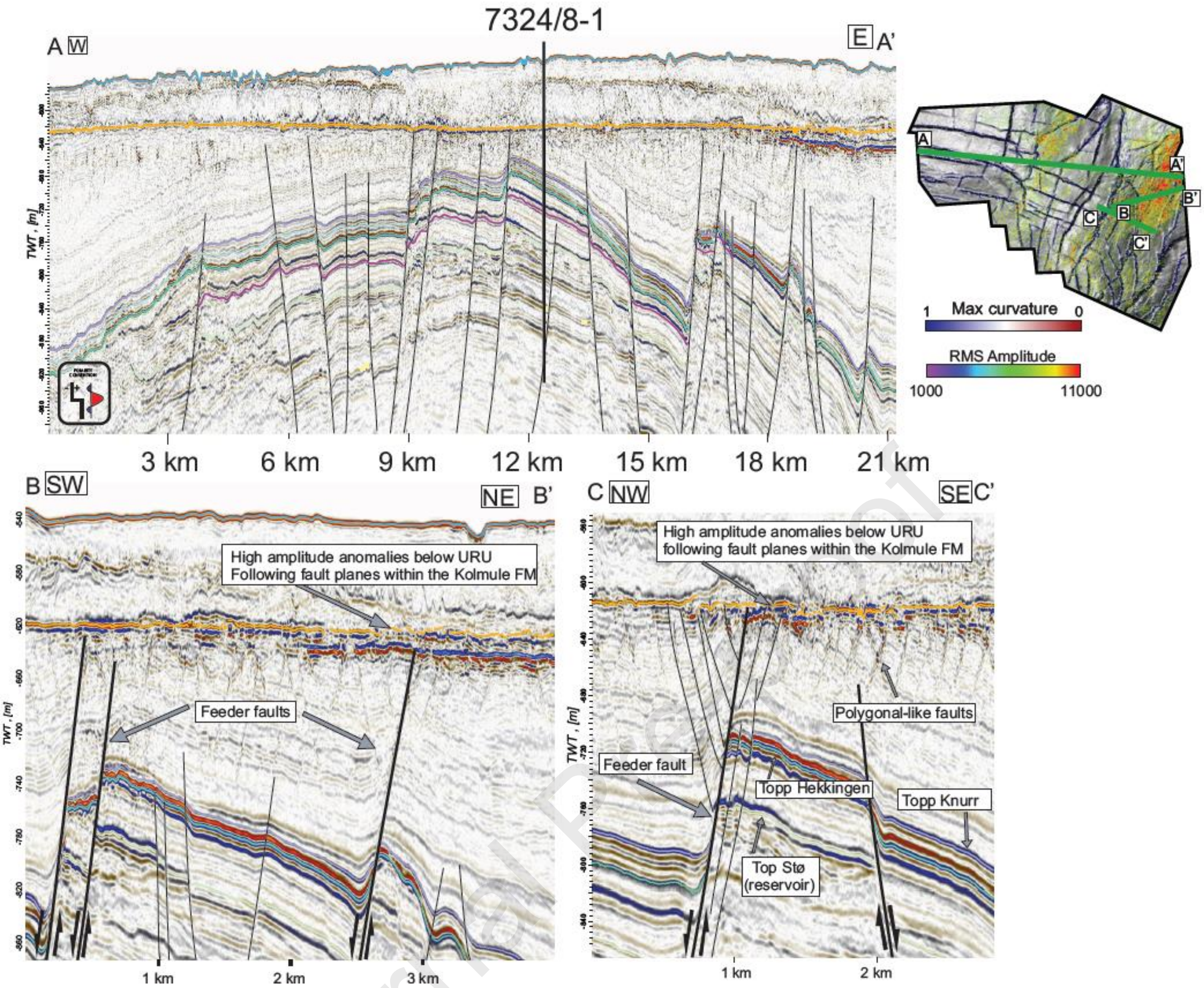


**Figure. 5** Seismic profile lines from the Wisting High-resolution P-cable seismic (HR14_3D_HFCE1). Inset map in the top right corner shows high-amplitude anomalies superimposed on a maximum curvature extraction of the top Hekkingen seismic horizon and location of profiles. Profile line A-A' showing the doming shape of the Wisting anticlinal structure and the location of well 7324/8-1. Profile line B-B' show the amplitude anomaly indicated on inset map, and potential feeder faults for fluid migration and accumulation of flids below the URU (orange line). Profile line C-C' demonstrates potential fluid distribution along the major fault planes and polygonal-like faults within the Kolmule Formation. Top Formations and associated colours are demonstrated in Fig. 2.

## 4.2 DlogR

Many of the wells in our study lack maturity data and TOC measurements, and the lithological characterisation is based on cuttings and core photos where this is available. In general, the Fuglen and Hekkingen formations are shale dominated with the latter usually considered a high TOC shale, this is further supported by gamma ray readings in both formations. However, the gamma ray is sensitive to other detrital components (e.g., feldspar, micas, glauconite etc.) and should not be used as a stand-alone tool for TOC estimates and/or lithology. Therefore, we have used DlogR to provide higher confidence that TOC does correlate to elevated gamma ray responses. Fig. 6 shows the DlogR values shown against gamma ray and acoustic-resistivity logs, respectively. The cumulative caprock interval includes both Fuglen and Hekkingen formations and the general depth and thickness is summarized in table 2. The DlogR is calculated at each depth increment corresponding to the wireline readings and the baseline values are taken from the overlay areas as indicated in Fig. 6. These are the more clay rich rocks with lower source-rock potential. In all cases this interval is found within the Fuglen Formation, and mostly in the lower parts, and in the Bjaaland well such is observed in both the Fuglen and Hekkingen interval. The upper section of Fig. 6 displays three of the Wisting wells, and the bottom line shows the Apollo, Atlantis, and Mercury wells. The Wisting well plots show good correlation between the gamma ray readings, and the Sonic and Resistivity crossover with calculated DlogR indicating higher TOC intervals with increased GR. This is especially visible in the Hekkingen Formation in the Hanssen well where the DlogR calculations fit well with both the GR spikes, and the sonic and resistivity overlay. In the Wisting Central well, the whole Hekkingen Formation tends towards generally higher TOC, while GR spikes in the Fuglen Formation correlates with increased DlogR, which also follows the crossover interval of the lower Fuglen Formation. The crossover in the Bjaaland well corresponds to both GR spikes and increased DlogR readings at 630 m (MD). The Apollo and Atlantis well show less prominent overlay of the resistivity and sonic velocity, but correlates well with increasing GR response, and individual GR spikes. Additionally, both Apollo and Atlantis have higher DlogR values in the upper 50m of the Fuglen Formation. Although the lower part of the Fuglen Formation in both Atlantis and Apollo wells show a separation below the baseline, this is not a crossover. The Mercury well shows the same trends with increased DlogR with crossover of sonic and resistivity and increasing GR readings, but also generally show elevated DlogR and a long interval from 675 md to 692,5 md with slight crossover.

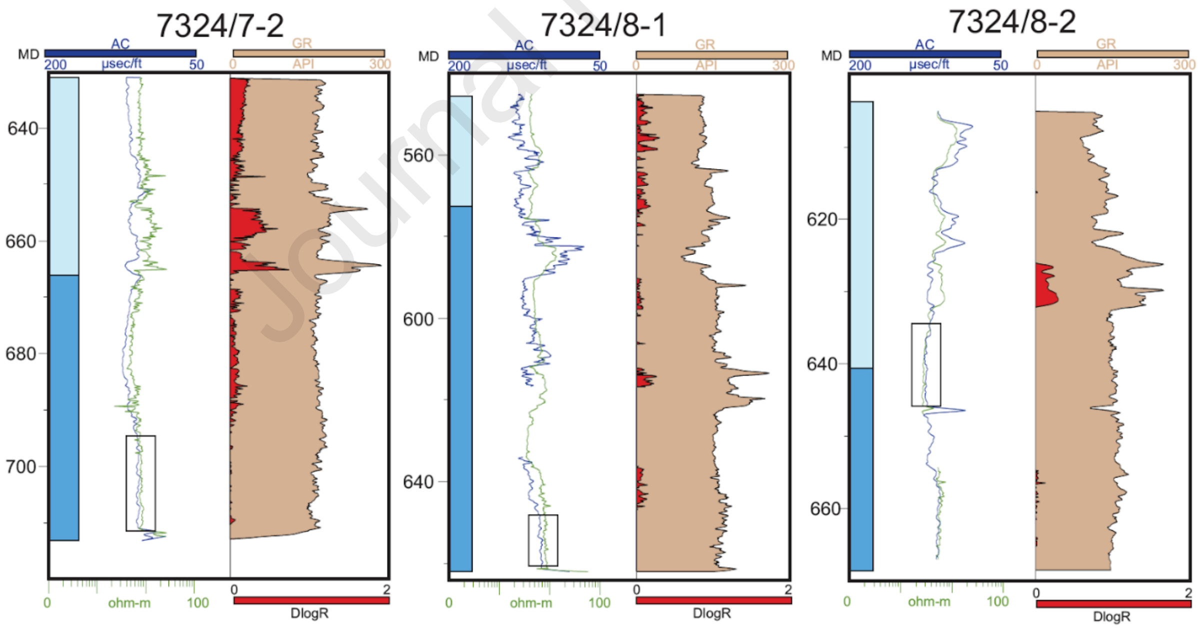

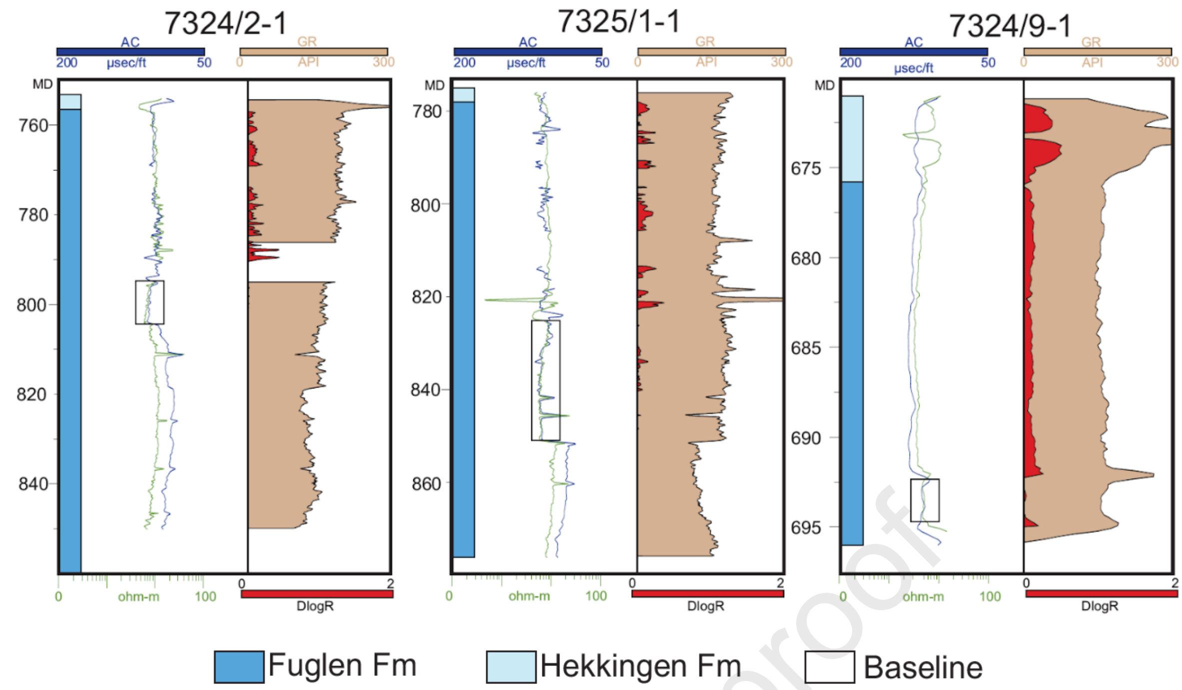


**Figure. 6** Log plot of the wells in the area with complete to nearly complete Sonic and Resistivity logs in the Fuglen and Hekkingen Formations. Top row: Hanssen (7324/7-2), Wisting I (7324/8-1) and Bjaaland (7324/8-2). Bottom row: Apollo (7324/2-1), Atlantis (7325/1-1) and 7324/9-1 (Mercury). The red log shows the DlogR calculations overlain the gamma ray readings from the wireline log (light brown). Baseline values are indicated by the black box on each well section.

### 4.3 Elastic properties and higher TOC intervals

The DlogR calculations show that there is a correlation between the gamma ray response in the wells and intervals with elevated TOC-levels. Crossplots of Young's modulus (E) and Poisson's ratio (v) are a useful tool for investigating how a rock interval might withstand deformation or fracture. All the wells in the area are considered to share similar burial history, although Wisting are located shallower compared to the other wells respectively. lower Young's Modulus and higher Poisson's ratio generally favour more ductile deformation implying that the rock may obtain more stress and strain before it fractures, on the contrary, higher E values and lower v points towards a more brittle domain. Naturally, only the wells with P and S-velocity readings are included. Wireline readings for either the Hekkingen or Fuglen formations are shown in the crossplots in Fig. 7 (a), (b), (c), (d) and (e), while crossplot (f) and (g) show the wells with individual colour code for easier separation. A linear relationship between both parameters are evident in Fig. 7 from the lower right corner to the top left corner. Crossplot (a) shows the calculated E and v for the Hekkingen formation, and that all wells plot in a cluster in the lower right corner. In the closeup (b) we see that Apollo has the highest E and v compared to the Hanssen and Bjaaland wells. The colour scale is directly linked to the API for each well and formation, and darker colour corresponds to higher API values. The linear trend is most clear for the Hanssen well, and the highest API readings have generally low E for all the wells. Bjaaland has slightly higher E values but also shows the lowest E values and highest v where the API readings are highest. Apollo deviates from the two latter with its thin Hekkingen interval (<3 m), High E, low v and high API readings.

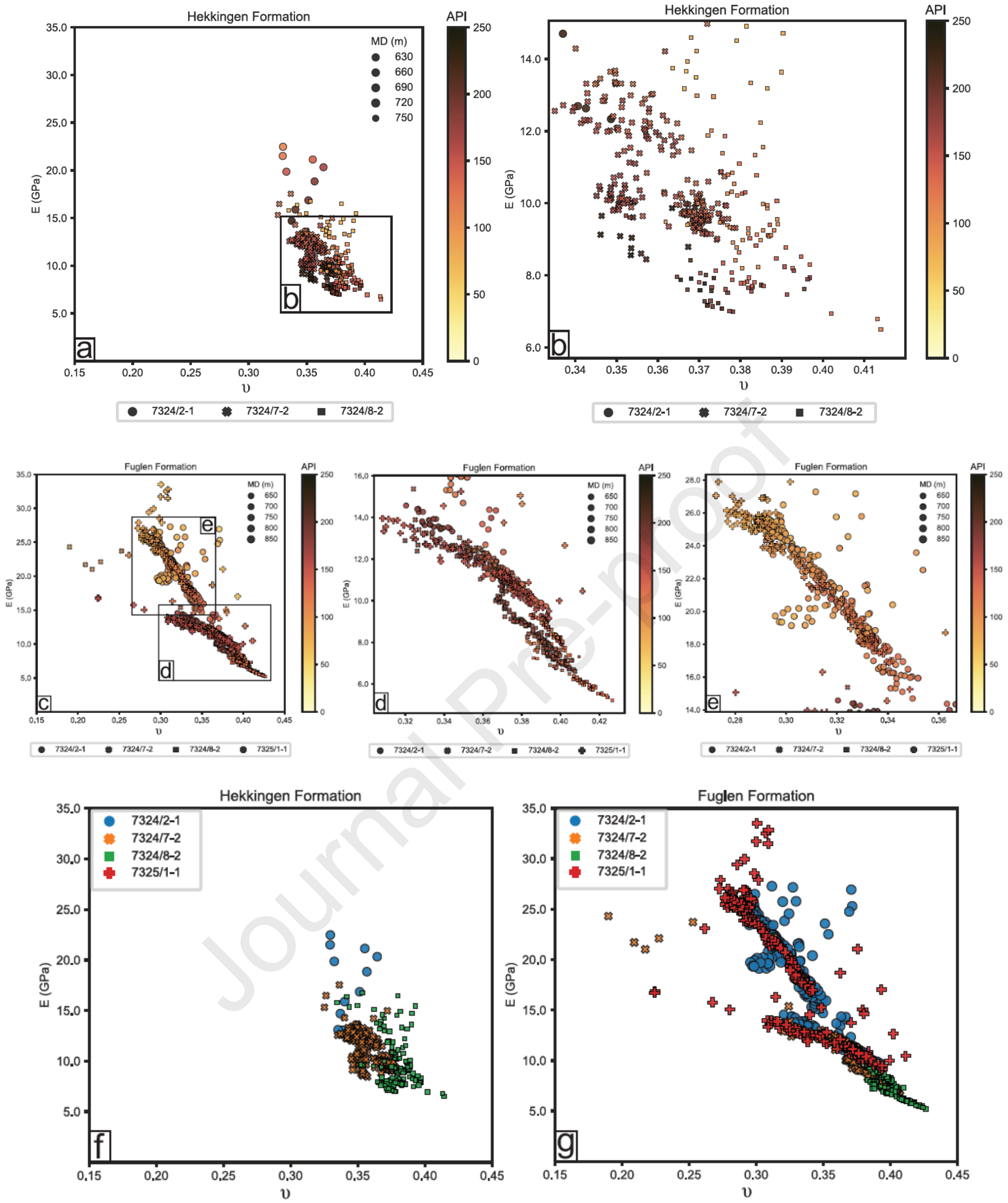


**Figure. 7** E-v crossplots demonstrating the linear relationship between the elastic parameters of Young's Modulus and Poisson's ratio of both the Fuglen and Hekkingen formations. (a) Hekkingen formation, (b) zoom in of Hekkingen Formation, (c) Fuglen Formation, (d) and (e) zoom in of Fuglen Formation. Crossplot (a) and © are colour coded according to their API readings respectively extracted from each well. (f) and (g) show the same crossplots as (a) and (c) however, colour coded according to each well and not by API.

In the Apollo well Poisson's ratio is generally lower in the Fuglen Formation than the Hekkingen Formation. In the Fuglen Formation crossplot, there are two different trends with various inclinations. The two different collections also have different colour variations within. Crossplot (d) shows a zoom in on the lower end with the less inclining trend, the darker colour shows elevated API readings compared to collection zoomed in on in crossplot (e). In the lower right corner in (d) we find the Bjaaland well accompanied with the Hanssen well, and the top half is dominated mainly by the Hanssen, Apollo and Atlantis wells. The zoom shown in crossplot (e) highlights the colour variation and change in inclination, and we see a clearly palening trend upwards corresponding to lower API readings. Comparing crossplot (e) with the well-colour coded crossplot (g) we see that the Bjaaland well is constrained to the lower right corner, and that the Hanssen well is mostly constrained to the lower half of the crossplot, with only a few deviating points off the two main trends. On the contrary both the Apollo and Atlantis well are strongly represented in both trends, only with a few deviation points above and sideways to the main collections.

### 4.4 Ductile/brittle response based on log-derived elastic parameters

Compacting sediments undergoing a reduction in porosity show a correlation between the Vp/Vs ratio and the density of the rock. In general, the higher the Vp/Vs and the lower the Young's Modulus the more compliant the shale is expected to be. The Vp/Vs ratio is sensitive to changes in fluids, and in shales it can be used to identify intervals in the well with a better sealing capacity (Bailey and Dutton, 2012, Eastwood and Castagna, 1983, Guo et al., 2012).Fig. 7 demonstrated the trend within both the Fuglen and Hekkingen formations, and wells that show better seal integrity based on elastic response, the crossplots in Fig. 8 also show similar trends when comparing Vp/Vs and density. In the Hekkingen Formation, densities and Vp/Vs ratios range from 2.1 – 2.7 g/$cm^3$ and between 1.6 – 2.6 (Fig. 8a). The highest Vp/Vs ratio are observed in the Hanssen and Mercury well, which both have low Young's Modulus values.  But for the Apollo well, which has a 2 m thick Hekkingen Formation, the density is well within the range of 2.4 – 2.7 g/$cm^3$, and the Young's modulus increases with increased density. In fact, most wells show lower Young's Modulus values with decreasing density.

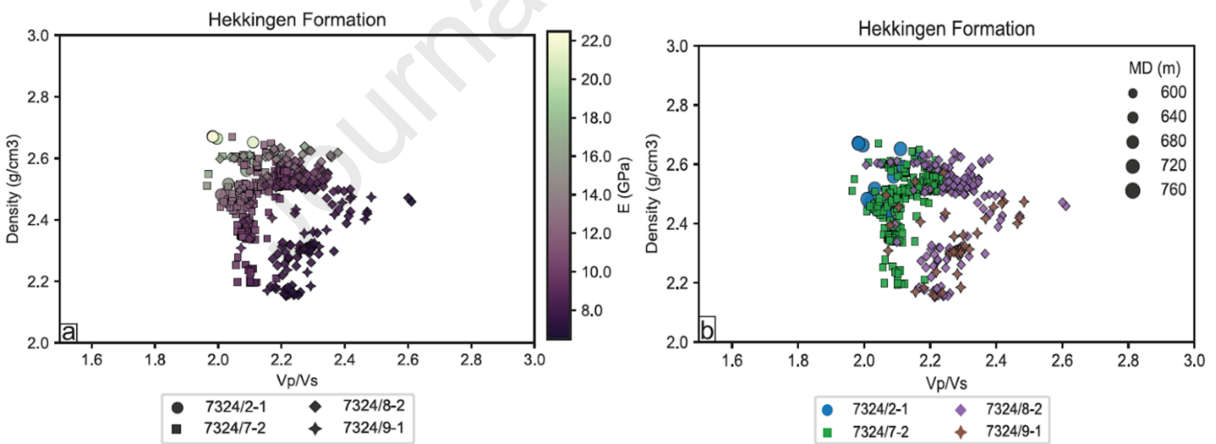

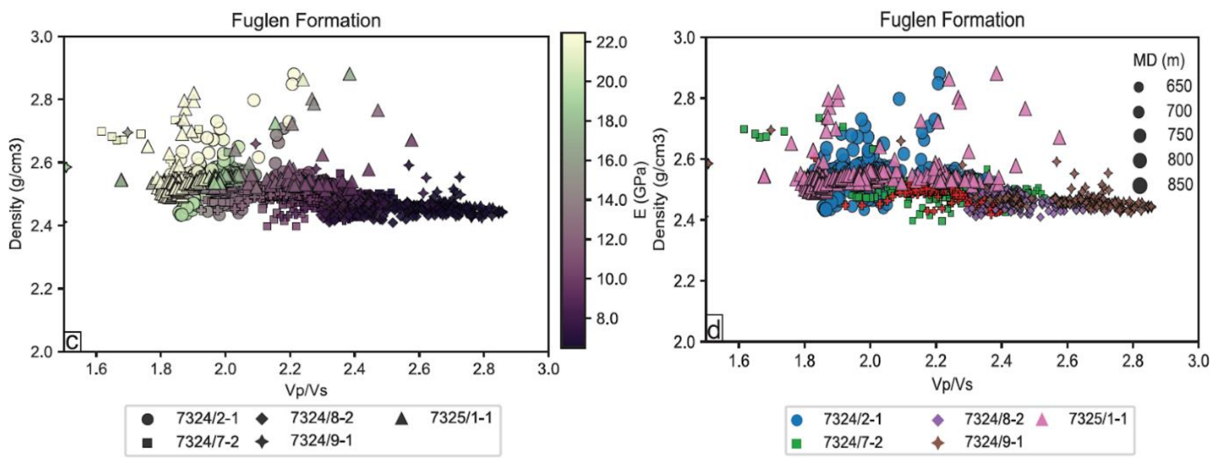


**Figure. 8** Density - Vp/Vs crossplots indicating correlation with shaly and sandy intervals within the Hekkingen (a and b) and Fuglen (b and c) formations. The colour code in plot (a) and (c) is related to the calculated Young's Modulus (E) and plot (b) and (d) highlight the location of each well in the crossplots.

If we compare the two formations in the Wisting and Apollo wells trends are more visible, and the Apollo well shares the same signature in the Hekkingen Formation as in the Fuglen Formation, although the Fuglen Formation is 93 m thick in the Apollo well.

### 4.5 Fracture pressures in the Fuglen Formation

When comparing our study area with other parts of the Barents Sea (Riis and Wolff, 2020)and most basins of the world, the tests in the Hoop area are unusually high (Fig 9). While FITs only provide a lower boundary to the rocks true fracture pressure, they are still close to, or above the lithostatic gradient (the pressure exerted by overlying rocks and fluids). LOTs consistently demonstrate leak-off pressures 25 to 60 bar above lithostatic. The XLOT at the

Atlantis well initial leak-off pressure is also similar, however, subsequent cycles show much lower pressures.

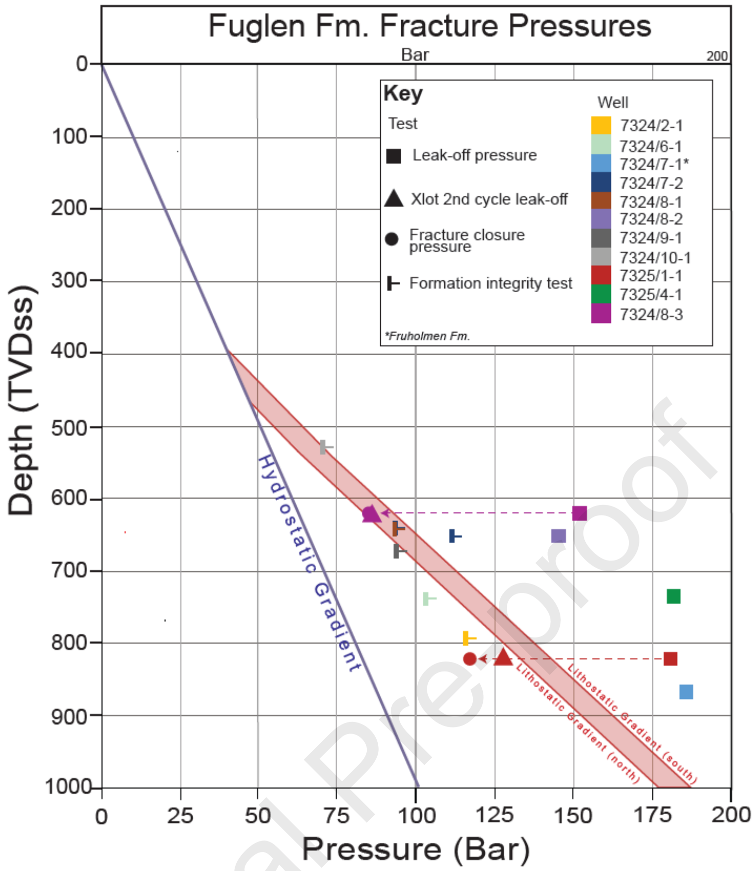


**Figure. 9** – Formation mechanical strength tests in the Greater Hoop area. Leak-off pressures are unusually high in the area, all of which greatly exceed the lithostatic pressure (vertical stress) indicating extremely high tensile strength.

## 4.6 Change in elasticity with depth

Fig. 10a and b illustrate the calculated Poisson's ratio vs depth in most of the wells (7324/7-1 and 7324/8-1 are not included in Fig. 10b, and 7324/71S is not included in Fig. 10a). The cross-plots illustrate the expected trend for both formations with decreasing Poisson's ratio with depth and increasing stress. The Wisting wells, including Hanssen and Bjaaland are located close together in the lower right corner for both Fig 10.a and b, mostly within 0.3 and 0.45. These are the wells with the highest uplift on the Wisting anticline and located on the crest of the Wisting structure (Fig. 4 and 5). For the Fuglen Formation it is the deeper Apollo and Atlantis wells that show the greatest variety with increasing depth. Their close-by location is coherent with them overlapping each other in Fig. 10a. They both share an overlapping fluctuating trend, closely related to the heterogeneity in the shales interpreted through the well logs. The 7325/4-1 Gemini Nord well has a surprisingly wide range of values throughout the whole well in both formations plotting from 0.15 to 0.35, albeit a bit lower on the scale compared to the Wisting wells. In the Mercury, Apollo and Atlantis wells the Hekkingen Formation is only between 3 and 4 m thick but still plot within a wide range with 0.3 – 0.35 for Atlantis, 0.34 – 0.37 for Apollo and 0.35 – 0.40 for Mercury.

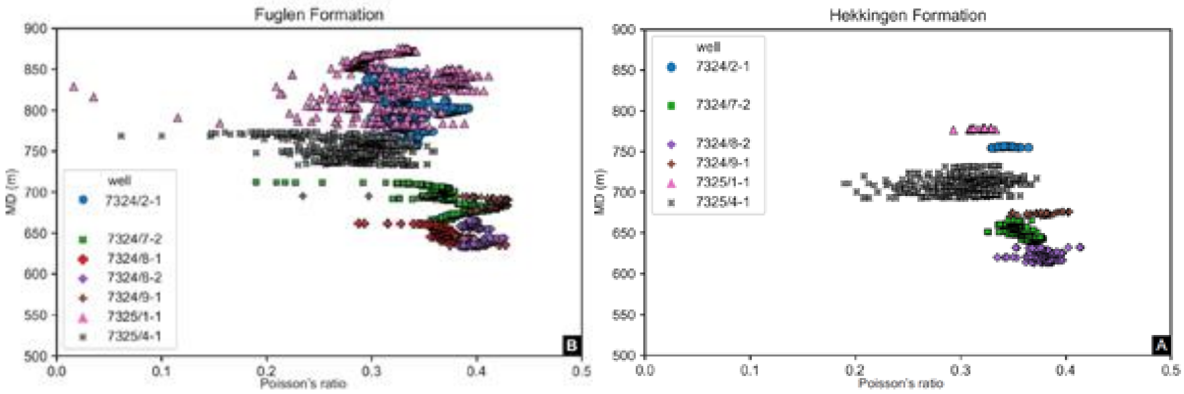


**Figure. 10** MD-v crossplot demonstrating the effect of increased stress (burial) on the elasticity.

The Fuglen Formation in well 7324/8-1, 7324/8-2, 7324/9-1, and upper parts of well 7325/1-1 show the lowest Poisson's ratio values. The Atlantis well show a deviating trend where the upper most part show lower Poisson's ratio values compared to the lower part of the formation that show lower Poisson's ratio and higher Young's Modulus. The Atlantis and Apollo wells obey a similar correlation with respect to depth. Lower parts of the unit show more brittle response, while upper parts appear more ductile.

## 5. Discussion

### 5.1 TOC vs GR

Previous studies have demonstrated a good correlation between TOC and gamma ray in well logs in the Jurassic mudstones regionally on the Barents shelf (Cedeño et al., 2019, Senger et al., 2020, Hansen et al., 2020, Dypvik et al., 2010). However, in the study area there is a lack of direct TOC data. To increase confidence in the correlation of we have used Passey's method (DlogR), which uses acoustic and resistivity data to identify TOC and has also had success in the Barents shelf (Cappuccio et al., 2020). Fig.6 shows that the Passey's method and gamma ray API are in good agreement and also show that the Hekkingen, unsurprisingly, exhibits stronger responses due to its higher TOC than the Fuglen formation throughout the Bare (Abay et al., 2014, Koevoets et al., 2016a, Koevoets et al., 2018a, Senger et al., 2020, Hansen et al., 2020, Dypvik et al., 2010). The intervals showing lower gamma ray and DlogR responses appear to correlate with zones of higher silt content in drill cuttings (NPD, 2020), though it is worth noting that cuttings depths are relatively uncertain.

### 5.2 Elasticity and TOC

Fig. 7 demonstrates that in the Fuglen and Hekkingen formations that the highest gamma ray values are correlate with the lowest Young's modulus and highest Poisson's ratio. This suggests that intervals of high TOC are the most ductile. On the other hand, lower gamma ray values correlate with higher Young's modulus and lower Poisson's ratio values and, thusly, more brittle. In Fig. 7c, there are two distinct trends. Geologically, this is likely due to sharp lithological changes between high TOC shales and more silica dominated intervals.

The Hekkingen Formation exhibits ductile properties in the south, while it thins and lacks data in the northern part of the study area. However, the Fuglen Formation, which directly overlies the reservoir throughout the study area, shows much more spatial heterogeneity. The Fuglen Formation in northern wells (Apollo and Atlantis) possess more brittle properties compared to the Wisting area. This can be explained by cuttings that show the Fuglen Formation becomes coarser towards the north in the study area (NPD, 2020)

The well with the most ductile properties in the cap rock is Bjaaland, which is situated on a rotated fault block. Despite this, structure was discovered to be water wet with a residual hydrocarbon column, indicating past leakage. This is probably due to the extremely high offset of the bounding fault (Fig. 5), where the reservoir has been juxtaposed against the Cretaceous Kolmule Formation, which in this area is relatively silty (Marín et al., 2017a)

### 5.3 Fractures and pore pressure

Although Young's modulus and Poisson's ratio are good indicators of sealing potential of a lithology, it is still possible that a seal can be mechanically compromised through fracturing. However, the leak-off test (LOT) and extended leak-off test (XLOT) data from the Fuglen Formation throughout the study area suggests it is unlikely.

The overall high leak-off pressures and the big differences in XLOT cycles clearly demonstrates that the Fuglen Formation possesses unusually high tensile strength (represented by dashed line in Fig. 9) considering its shallow depth. Such high leak-off pressures are undoubtedly due to previous burial, with subsequent recent uplift leaving the rocks overcompacted for their present-day depth. However, the fact that all wells in the study area display such high values, it also shows that the Fuglen Formation has remained remarkably strong despite uplift, at least at the well-bore locations, which is further confirmed by the XLOT data in the Atlantis and Wisting Central III wells (Fig 9). Although it is unreasonable to assume that there are no fracture zones in the cap rock over the entire structure, the LOT and XLOT data does show that the studied Fuglen interval in this paper is not fractured.

The Fuglen Formation possesses extremely good mechanical sealing potential as proven by the relatively the XLOT data. Even fracture closure pressures in the study area are approaching lithostatic (Fig. 9) and demonstrate even fractured intervals would require considerable pressure to be reopened. The formation pressure in the underlying Stø Formation reservoir is at hydrostatic throughout the study area, therefore there is a large window between the pore pressure and fracture pressure which could support hydrocarbon columns far in excess of structural closures (and residual hydrocarbon columns). Furthermore, due to overcompaction, the more clay dominated intervals are also unlikely to leak through capillary processes.

Because the rock possesses so much tensile strength, there is a possibility that leak-off driven fracturing is influenced more by the rock fabric than regional stress, in which

### 5.4 Faults

All available data indicates that the Fuglen and Hekkingen formations possess good sealing properties as top seals. However, the importance of faults became clear in 2016 at Wisting, where severe mud losses occurred across while drilling through faults in a horizontal appraisal well (7324/7-3s) (NPD, 2020). Seismic data also show that there is potential leakage in the area as demonstrated in Fig. 5. There are high amplitude anomalies directly above the fault crests and along fault planes within the Kolmule Formation that may be indicative of leakage.

Considering that the Bjaaland well exhibits some of the best elastic properties in the Fuglen and Hekkingen formations in our study area yet still only showed residual oil column may point towards that it has a fault problem. The large high-amplitude anomaly visualized in Fig 5 seismic section and inset map, follows the delimiting fault at the Bjaaland prospect. Taking into account the four-way structure of the Wisting anticline, and its location sandwiched between the HFC and the Maud Basin the stress-fields may deviate from the Bjarmeland Platform area, and certain fault orientations may favour leakage at this location. In addition, the Bjaaland was drilled on the structure with the highest fault throw observed in the seismic data, offsetting the Stø Formation (reservoir) to the overlying Kolmule Formation.

### 5.5 Sealing potential

The overall sealing potential of the study area appears to be greatest in the south and diminish towards the north. The Hekkingen Formation displays favourable elastic properties, but pinches out to the north. The Fuglen Formation is greater than 30 metres thick throughout the area, but appears to be more brittle in the north, due to higher silt content. This may explain why the Apollo well had oil shows, but no hydrocarbons retained. On the contrary the southern wells shows good sealing properties, including the technical gas discovery in the Gemini Nord (also minor oil discovery), Mercury well and the oil discoveries of Wisting and Hanssen. The exception to this is the Bjaaland prospect that contained a residual hydrocarbon column despite exhibiting the best rock mechanical properties of all wells in our study area, but as mentioned suffers from fault leakage.

## 6. Conclusion

Because the northern Barents has undergone a series of uplift events throughout the Cenozoic, it is critical to assess the mechanical properties of the Jurassic caprocks in the area. This is particularly the case in the Greater Hoop area where the Jurassic shales are the last line of defence to the seabed. In this contribution we demonstrate some regional variability in the caprock sealing potential based on rock mechanics data. We show that the Fuglen Formation caprock has retained its strength throughout uplift and could retain a hydrocarbon column far in excess of any observed residual columns or structural closures.

Despite the fact that the Wisting area possesses some of the shallowest (to seabed) reservoirs in the world, it appears that the caprock is remarkably intact and competent. However, faults in the area are clearly a major risk to hydrocarbon retention and must be assessed on a prospect scale.

Caprock shales possess favourable sealing properties based on rock mechanical data. While the Hekkingen For does exhibit better properties, likely due to elevated TOC, the Fuglen still shows favourable sealing properties. This is highlighted by LOTs and XLOTs which show it has retained its tensile strength during uplift.

## Declaration of competing interests

The authors declare that they have no known competing financial interests or personal relationships that could have appeared to influence the work reported in this paper.

## CRediT author contribution statement

**Renate Paulsen:** Conceptualization, Methodology, Formal Analysis, Investigation, Data Curation, Writing – Original Draft, Writing – Review & Editing, Project Administration, Visualization **Thomas Birchall:** Conceptualization, Methodology, Writing – Review & Editing **Kim Senger:** Writing – Review & Editing **Sten-Andreas Grundvåg:** Writing – Review & Editing


## Acknowledgements

This research is funded by ARCEx, the Research Centre for Arctic Petroleum Exploration, which is funded by the Research Council of Norway (grant no. 228107). The authors sincerely appreciate access to seismic data through TGS, well-data from the DISKOS database (https://www.npd.no/en/diskos/) administered by the Norwegian Petroleum Directorate (NPD) and academic licenses for Petrel at the University of Tromsø and UNIS. Additionally, we would like to thank OMV Norge and Equinor for their valuable input and access to in-house data. Lastly the author would like to thank Peter Betlem at UNIS for his valuable help with implementing the scrips into crossplots.


## References


ABAY, T. B., KARLSEN, D. A. & PEDERSEN, J. H. 2014. Source rocks at Svalbard: an overview of Jurassic and Triassic formations and comparison with offshore Barents Sea time equivalent source rock formations. *AAPG Datapages Search and Discovery Article*, 30372.

ABAY, T. B., KARLSEN, D. A., PEDERSEN, J. H., OLAUSSEN, S. & BACKER-OWE, K. 2018. Thermal maturity, hydrocarbon potential and kerogen type of some Triassic–Lower Cretaceous sediments from the SW Barents Sea and Svalbard. *Petroleum Geoscience,* 24**,** 349-373.

AMANTOV, A., FJELDSKAAR, W. & CATHLES, L. 2011. Glacial erosion/sedimentation of the Baltic region and the effect on the postglacial uplift. *The Baltic sea basin.* Springer.

BAIG, I., FALEIDE, J. I., JAHREN, J. & MONDOL, N. H. 2016. Cenozoic exhumation on the southwestern Barents Shelf: Estimates and uncertainties constrained from compaction and thermal maturity analyses. *Marine and Petroleum Geology,* 73**,** 105-130.

BAIG, I., FALEIDE, J. I., MONDOL, N. H. & JAHREN, J. 2019. Burial and exhumation history controls on shale compaction and thermal maturity along the Norwegian North Sea basin margin areas. *Marine and Petroleum Geology,* 104**,** 61-85.

BAILEY, T. & DUTTON, D. An empirical Vp/Vs shale trend for the Kimmeridge Clay of the Central North Sea. 74th EAGE Conference and Exhibition incorporating EUROPEC 2012, 2012. European Association of Geoscientists & Engineers, cp-293-00400.

BERNDT, C., BÜNZ, S. & MIENERT, J. 2003. Polygonal fault systems on the mid-Norwegian margin: a long-term source for fluid flow. *Geological Society, London, Special Publications,* 216**,** 283-290.

BIRCHALL, T., SENGER, K., HORNUM, M., OLAUSSEN, S. & BRAATHEN, A. 2020a. Underpressure in the northern Barents shelf: Causes and implications for hydrocarbon exploration. *AAPG Bulletin*.

BIRCHALL, T., SENGER, K., HORNUM, M. T., OLAUSSEN, S. & BRAATHEN, A. 2020b. Underpressure in the northern Barents shelf: Causes and implications for hydrocarbon exploration. *AAPG Bulletin,* 104**,** 2267-2295.

BJORLYKKE, K. 2010. *Petroleum geoscience: From sedimentary environments to rock physics*, Springer Science & Business Media.

BJØRLYKKE, K. 1993. Fluid flow in sedimentary basins. *Sedimentary Geology*, 86**,** 137-158.

BUKAR, M., WORDEN, R. H., BUKAR, S. & SHELL, P. 2020. Diagenesis and its controls on reservoir quality of the Tambar oil field, Norwegian North Sea. *Energy Geoscience*, 2**,** 10-31.

CAPPUCCIO, F., PORRECA, M., OMOSANYA, K., MINELLI, G. & HARISHIDAYAT, D. 2020. Total organic carbon (TOC) enrichment and source rock evaluation of the Upper Jurassic-Lower Cretaceous rocks (Barents Sea) by means of geochemical and log data. *International Journal of Earth Sciences*, 110.

CARCIONE, J. M., GUREVICH, B. & CAVALLINI, F. 2000. A generalized Biot–Gassmann model for the acoustic properties of shaley sandstones1. *Geophysical Prospecting*, 48**,** 539-557.

CAVANAGH, A. J., DI PRIMIO, R., SCHECK-WENDEROTH, M. & HORSFIELD, B. J. J. O. T. G. S. 2006. Severity and timing of Cenozoic exhumation in the southwestern Barents Sea. 163**,** 761-774.

CEDEÑO, A., OHM, S. & ESCALONA, A. Facies Variations Within the Hekkingen Formation: An Interdisciplinary Approach. 29th International Meeting on Organic Geochemistry, 2019. European Association of Geoscientists & Engineers, 1-2.

COLLANEGA, L., MASSIRONI, M., BREDA, A. & KJØLHAMAR, B. E. 2017. Onset of N-Atlantic rifting in the Hoop Fault Complex (SW Barents Sea): An orthorhombic dominated faulting? *Tectonophysics*, 706**,** 59-70.

DAVIS, G. H., REYNOLDS, S. J. & KLUTH, C. F. 2011. *Structural geology of rocks and regions*, John Wiley & Sons.

DIMAKIS, P., BRAATHEN, B. I., FALEIDE, J. I., ELVERHØI, A. & GUDLAUGSSON, S. T. J. T. 1998. Cenozoic erosion and the preglacial uplift of the Svalbard–Barents Sea region. 300**,** 311-327.

DORÉ, A. 1995. Barents Sea geology, petroleum resources and commercial potential. *Arctic***,** 207-221.

DORÉ, A., CORCORAN, D. & SCOTCHMAN, I. 2002. Prediction of the hydrocarbon system in exhumed basins, and application to the NW European margin. *Geological Society, London, Special Publications*, 196**,** 401-429.

DORÉ, A., SCOTCHMAN, I. & CORCORAN, D. J. J. O. G. E. 2000. Cenozoic exhumation and prediction of the hydrocarbon system on the NW European margin. 69**,** 615-618.

DURAN, E. R., DI PRIMIO, R., ANKA, Z., STODDART, D. & HORSFIELD, B. 2013. 3D-basin modelling of the Hammerfest Basin (southwestern Barents Sea): A quantitative assessment of petroleum generation, migration and leakage. *Marine and petroleum geology*, 45**,** 281-303.

DYPVIK, H., NAGY, J., EIKELAND, T., BACKER-OWE, K. & JOHANSEN, H. J. S. G. 1991. Depositional conditions of the Bathonian to Hauterivian Janusfjellet subgroup, Spitsbergen. 72**,** 55-78.

DYPVIK, H., SMELROR, M., MØRK, A., WERNER, S. C. & TORSVIK, T. H. 2010. Impact Cratering and Post-impact Sedimentation. *The Mjølnir Impact Event and its Consequences.* Springer.

DÖRR, N., LISKER, F., CLIFT, P., CARTER, A., GEE, D. G., TEBENKOV, A. & SPIEGEL, C. 2012. Late Mesozoic–Cenozoic exhumation history of northern Svalbard and its regional significance: Constraints from apatite fission track analysis. *Tectonophysics*, 514**,** 81-92.

EASTWOOD, R. L. & CASTAGNA, J. P. Basis for interpretation of Vp/Vs ratios in complex lithologies. SPWLA 24th Annual Logging Symposium, 1983. Society of Petrophysicists and Well-Log Analysts.

EDMUNDSON, I., ROTEVATN, A., DAVIES, R., YIELDING, G. & BROBERG, K. 2020. Key controls on hydrocarbon retention and leakage from structural traps in the Hammerfest Basin, SW Barents Sea: implications for prospect analysis and risk assessment. *Petroleum Geoscience*, 26**,** 589-606.

FALEIDE, J. I., TSIKALAS, F., BREIVIK, A. J., MJELDE, R., RITZMANN, O., ENGEN, O., WILSON, J. & ELDHOLM, O. J. E. 2008. Structure and evolution of the continental margin off Norway and the Barents Sea. 31**,** 82-91.

FALEIDE, J. I., VÅGNES, E. & GUDLAUGSSON, S. T. 1993a. Late Mesozoic-Cenozoic evolution of the south-western Barents Sea in a regional rift-shear tectonic setting. *Marine and Petroleum Geology,* 10**,** 186-214.

FALEIDE, J. I., VÅGNES, E., GUDLAUGSSON, S. T. J. M. & GEOLOGY, P. 1993b. Late Mesozoic-Cenozoic evolution of the south-western Barents Sea in a regional rift-shear tectonic setting. 10**,** 186-214.

GABRIELSEN, P. T., PEDERSEN, C. B., FANAVOLL, S. & KJØLHAMAR, B. E. Integration of Seismic and 3D CSEM Data De-risks Play Models in the Hoop Area, Barents Sea. OTC Arctic Technology Conference, 2015. Offshore Technology Conference.

GABRIELSEN, R., GRUNNALEITE, I. & OTTESEN, S. 1993. Reactivation of fault complexes in the Loppa High area, southwestern Barents Sea. *Norwegian Petroleum Society Special Publications.* Elsevier.

GABRIELSEN, R. & KLØVJAN, O. 1997. Late Jurassic-early Cretaceous caprocks of the southwestern Barents Sea: Fracture systems and rock mechanical properties. *In:* P. MØLLER-PEDERSEN, A. G. K. (ed.) *Hydrocarbon Seals–Importance for Exploration Production.* Norwegian Petroleum Society, Special Publications.

GABRIELSEN, R. H., FAERSETH, R. B. & JENSEN, L. N. 1990a. Structural elements of the Norwegian continental shelf. Pt. 1. The Barents Sea region. NPD-Bulletin NO 6**,** 34pp.

GABRIELSEN, R. H., FAERSETH, R. B. & JENSEN, L. N. 1990b. *Structural elements of the Norwegian continental shelf. Pt. 1. The Barents Sea region*, Norwegian Petroleum Directorate.

GABRIELSEN, R. H., SOKOUTIS, D., WILLINGSHOFER, E. & FALEIDE, J. I. 2016. Fault linkage across weak layers during extension: an experimental approach with reference to the Hoop Fault Complex of the SW Barents Sea. *Petroleum Geoscience,* 22**,** 123-135.

GERNIGON, L., BRÖNNER, M., ROBERTS, D., OLESEN, O., NASUTI, A. & YAMASAKI, T. 2014. Crustal and basin evolution of the southwestern Barents Sea: From Caledonian orogeny to continental breakup. *Tectonics,* 33**,** 347-373.

GLØRSTAD-CLARK, E., FALEIDE, J. I., LUNDSCHIEN, B. A. & NYSTUEN, J. P. 2010. Triassic seismic sequence stratigraphy and paleogeography of the western Barents Sea area. 27**,** 1448-1475.

GRIESER, W. V. & BRAY, J. M. Identification of production potential in unconventional reservoirs. Production and Operations Symposium, 2007. Society of Petroleum Engineers.

GRUNDVÅG, S.-A., MARIN, D., KAIRANOV, B., ŚLIWIŃSKA, K., NØHR-HANSEN, H., JELBY, M. E., ESCALONA, A., OLAUSSEN, S. J. M. & GEOLOGY, P. 2017. The Lower Cretaceous succession of the northwestern Barents Shelf: Onshore and offshore correlations. 86**,** 834-857.

GUDLAUGSSON, S., FALEIDE, J., JOHANSEN, S., BREIVIK, A. J. M. & GEOLOGY, P. 1998. Late Palaeozoic structural development of the south-western Barents Sea. 15**,** 73-102.

GUO, Z., CHAPMAN, M. & LI, X. 2012. A shale rock physics model and its application in the prediction of brittleness index, mineralogy, and porosity of the Barnett Shale. *SEG technical program expanded abstracts 2012.* Society of Exploration Geophysicists.

HANSEN, J. A., MONDOL, N. H., TSIKALAS, F. & FALEIDE, J. I. 2020. Caprock characterization of Upper Jurassic organic-rich shales using acoustic properties, Norwegian Continental Shelf. *Marine and Petroleum Geology,* 121**,** 104603.

HENRIKSEN, E., BJØRNSETH, H., HALS, T., HEIDE, T., KIRYUKHINA, T., KLØVJAN, O., LARSSEN, G., RYSETH, A., RØNNING, K. & SOLLID, K. 2011. Uplift and erosion of the greater Barents Sea: impact on prospectivity and petroleum systems. *Geological Society, London, Memoirs,* 35**,** 271-281.

HENRIKSEN, E., BJØRNSETH, H., HALS, T., HEIDE, T., KIRYUKHINA, T., KLØVJAN, O., LARSSEN, G., RYSETH, A., RØNNING, K. & SOLLID, K. 2011b. Uplift and erosion of the greater Barents Sea: impact on prospectivity and petroleum systems. 35**,** 271-281.

HENRIKSEN, E., RYSETH, A., LARSSEN, G., HEIDE, T., RØNNING, K., SOLLID, K. & STOUPAKOVA, A. J. G. S., LONDON, MEMOIRS 2011a. Tectonostratigraphy of the greater Barents Sea: implications for petroleum systems. 35**,** 163-195.

HERMANRUD, C., HALKJELSVIK, M. E., KRISTIANSEN, K., BERNAL, A. & STRÖMBÄCK, A. C. 2014a. Petroleum column-height controls in the western Hammerfest Basin, Barents Sea. *Petroleum Geoscience,* 20**,** 227-240.

HERMANRUD, C., HALKJELSVIK, M. E., KRISTIANSEN, K., BERNAL, A. & STRÖMBÄCK, A. C. 2014b. Petroleum column-height controls in the western Hammerfest Basin, Barents Sea.

HUUSE, M. & MICKELSON, M. 2004. Eocene sandstone intrusions in the Tampen Spur area (Norwegian North Sea Quad 34) imaged by 3D seismic data. *Marine and Petroleum Geology,* 21**,** 141-155.

INGRAM, G., URAI, J. & NAYLOR, M. 1997. Sealing processes and top seal assessment. *Norwegian Petroleum Society Special Publications.* Elsevier.

JAKOBSSON, M., MAYER, L., COAKLEY, B., DOWDESWELL, J. A., FORBES, S., FRIDMAN, B., HODNESDAL, H., NOORMETS, R., PEDERSEN, R. & REBESCO, M. 2012. The international bathymetric chart of the Arctic Ocean (IBCAO) version 3.0. *Geophysical Research Letters,* 39**,** 1-6.

KARLSEN, D. & SKEIE, J. 2006. Petroleum migration, faults and overpressure, part I: calibrating basin modelling using petroleum in traps—a review. *Journal of Petroleum Geology,* 29**,** 227-256.

KNUTSEN, S.-M. & LARSEN, K. 1997. The late Mesozoic and Cenozoic evolution of the Sørvestsnaget Basin: a tectonostratigraphic mirror for regional events along the Southwestern Barents Sea margin? *Marine and petroleum geology,* 14**,** 27-54.

KOEVOETS, M., ABAY, T., HAMMER, Ø. & OLAUSSEN, S. 2016a. High-resolution organic carbon–isotope stratigraphy of the Middle Jurassic–Lower Cretaceous Agardhfjellet Formation of central Spitsbergen, Svalbard. *Palaeogeography, Palaeoclimatology, Palaeoecology,* 449**,** 266-274.

KOEVOETS, M., ABAY, T., HAMMER, Ø. & OLAUSSEN, S. J. P., PALAEOCLIMATOLOGY, PALAEOECOLOGY 2016b. High-resolution organic carbon–isotope stratigraphy of the Middle Jurassic–Lower Cretaceous Agardhfjellet Formation of central Spitsbergen, Svalbard. 449**,** 266-274.

KOEVOETS, M. J., HAMMER, Ø., OLAUSSEN, S., SENGER, K. & SMELROR, M. 2018a. Integrating subsurface and outcrop data of the Middle Jurassic to Lower Cretaceous Agardhfjellet Formation in central Spitsbergen. *Norsk Geologisk Tidsskrift,* 98.

KOEVOETS, M. J., HAMMER, Ø., OLAUSSEN, S., SENGER, K. & SMELROR, M. J. N. J. O. G. 2018b. Integrating subsurface and outcrop data of the Middle Jurassic to Lower Cretaceous Agardhfjellet Formation in central Spitsbergen. 98**,** 1-34.

KTENAS, D., HENRIKSEN, E., MEISINGSET, I., NIELSEN, J. K. & ANDREASSEN, K. 2017. Quantification of the magnitude of net erosion in the southwest Barents Sea using sonic velocities and compaction trends in shales and sandstones. *Marine and Petroleum Geology,* 88**,** 826-844.

KTENAS, D., MEISINGSET, I., HENRIKSEN, E. & NIELSEN, J. K. 2018. Estimation of net apparent erosion in the southwestern Barents Sea by applying velocity inversion analysis. *Petroleum Geoscience***,** petgeo2018-002.

LASABUDA, A., LABERG, J. S., KNUTSEN, S.-M. & SAFRONOVA, P. 2018. Cenozoic tectonostratigraphy and pre-glacial erosion: A mass-balance study of the northwestern Barents Sea margin, Norwegian Arctic. *Journal of Geodynamics,* 119**,** 149-166.

LEE, M. W. 2002a. Modified Biot-Gassmann theory for calculating elastic velocities for unconsolidated and consolidated sediments. *Marine Geophysical Researches,* 23**,** 403-412.

LEE, M. W. 2002b. Modified Biot-Gassmann theory for calculating elastic velocities for unconsolidated and consolidated sediments. *Marine Geophysical Researches,* 23**,** 403-412.

LØSETH, H., WENSAAS, L., GADING, M., DUFFAUT, K. & SPRINGER, M. 2011. Can hydrocarbon source rocks be identified on seismic data? *Geology,* 39**,** 1167-1170.

LØTVEIT, I. F., FJELDSKAAR, W. & SYDNES, M. 2019. Tilting and flexural stresses in basins due to glaciations—An example from the Barents Sea. *Geosciences,* 9**,** 474.

MAKURAT, A., TORUDBAKKEN, B., MONSEN, K. & RAWLINGS, C. 1992. Cenezoic uplift and caprock seal in the Barents Sea: fracture modelling and seal risk evaluation. *SPE Annual Technical Conference and Exhibition*.

MARÍN, D., ESCALONA, A., ŚLIWIŃSKA, K. K., NØHR-HANSEN, H. & MORDASOVA, A. 2017a. Sequence stratigraphy and lateral variability of Lower Cretaceous clinoforms in the southwestern Barents Sea. *AAPG Bulletin,* 101**,** 1487-1517.

MARÍN, D., ESCALONA, A., ŚLIWIŃSKA, K. K., NØHR-HANSEN, H. & MORDASOVA, A. J. A. B. 2017b. Sequence stratigraphy and lateral variability of Lower Cretaceous clinoforms in the southwestern Barents Sea. 101**,** 1487-1517.

MARÍN, D., HELLEREN, S., ESCALONA, A., OLAUSSEN, S., CEDEÑO, A., NØHR- HANSEN, H. & OHM, S. 2020. The Middle Jurassic to lowermost Cretaceous in the SW Barents Sea: Interplay between tectonics, coarse- grained sediment supply and organic matter preservation. *Basin Research*.

MATHIA, E., RATCLIFFE, K. & WRIGHT, M. Brittleness Index-A Parameter to Embrace or Avoid? Unconventional Resources Technology Conference, San Antonio, Texas, 1-3 August 2016, 2016. Society of Exploration Geophysicists, American Association of Petroleum …, 1156-1165.

MATHIA, E. & RATCLIFFE, K. W., M 2016. Brittleness Index – A Parameter to Embrace or Avoid? *Unconventional Resources Technology Conference.* San Antonio, Texas.

MONDOL, N. H. 2018. Seal quality prediction using E-Poisson's ratio rock physics templet-A case study from the Norwegian Barents Sea. *GeoConvention*.

MÜLLER, R., KLAUSEN, T. G., FALEIDE, J. I., OLAUSSEN, S., EIDE, C. H. & SUSLOVA, A. 2019. Linking regional unconformities in the Barents Sea to compression-induced forebulge uplift at the Triassic-Jurassic transition. *Tectonophysics,* 765**,** 35-51.

NOORAIEPOUR, M., MONDOL, N. H., HELLEVANG, H. & BJØRLYKKE, K. 2017. Experimental mechanical compaction of reconstituted shale and mudstone aggregates: Investigation of petrophysical and acoustic properties of SW Barents Sea cap rock sequences. *Marine and Petroleum Geology,* 80**,** 265-292.

NPD. 2017. *Geological assessment of petroleum resources in the eastern part of Barents Sea North 2017* [Online]. Available: https://factpages.npd.no/ [Accessed 2020].

NPD. 2020. *NPD Fact Pages* [Online]. https://www.npd.no/en/facts/factpages/. Available: http://gis.npd.no/factmaps/html_21/ [Accessed 15.09.20].

OHM, S. E., KARLSEN, D. A. & AUSTIN, T. 2008a. Geochemically driven exploration models in uplifted areas: Examples from the Norwegian Barents Sea. *AAPG bulletin,* 92**,** 1191-1223.

OHM, S. E., KARLSEN, D. A. & AUSTIN, T. J. A. B. 2008b. Geochemically driven exploration models in uplifted areas: Examples from the Norwegian Barents Sea. 92**,** 1191-1223.

OLSEN, H., BRIEDIS, N. A. & RENSHAW, D. 2017. Sedimentological analysis and reservoir characterization of a multi-darcy, billion barrel oil field–The Upper Jurassic shallow marine sandstones of the Johan Sverdrup field, North Sea, Norway. *Marine and Petroleum Geology,* 84**,** 102-134.

OSTANIN, I., ANKA, Z., DI PRIMIO, R. & BERNAL, A. J. M. G. 2012. Identification of a large Upper Cretaceous polygonal fault network in the Hammerfest basin: Implications on the reactivation of regional faulting and gas leakage dynamics, SW Barents Sea. 332**,** 109-125.

PASSEY, Q., CREANEY, S., KULLA, J., MORETTI, F. & STROUD, J. 1990. A practical model for organic richness from porosity and resistivity logs. *AAPG bulletin,* 74**,** 1777-1794.

PEREZ ALTAMAR, R. & MARFURT, K. J. 2015. Identification of brittle/ductile areas in unconventional reservoirs using seismic and microseismic data: Application to the Barnett Shale. *Interpretation,* 3**,** T233-T243.

RICKMAN, R., MULLEN, M. J., PETRE, J. E., GRIESER, W. V. & KUNDERT, D. A practical use of shale petrophysics for stimulation design optimization: All shale plays are not clones of the Barnett Shale. SPE annual technical conference and exhibition, 2008. Society of Petroleum Engineers.

RIIS, F. & HALLAND, E. 2014. CO2 Storage Atlas of the Norwegian Continental Shelf: Methods Used to Evaluate Capacity and Maturity of the CO2 Storage Potential. *Energy Procedia,* 63**,** 5258-5265.

RIIS, F. & WOLFF, A. 2020. Use of Pore pressure data from the Norwegian continental shelf to characterize fluid-flow processes in geological timescales. *Geological Society, London, Special Publications,* 495.

RONNEVIK, H., BESKOW, B. & JACOBSEN, H. P. 1982. Structural and stratigraphic evolution of the Barents Sea.

SENGER, K., BIRCHALL, T., BETLEM, P., OGATA, K., OHM, S., OLAUSSEN, S. & PAULSEN, R. S. 2020. Resistivity of reservoir sandstones and organic rich shales on the Barents Shelf: Implications for interpreting CSEM data. *Geoscience Frontiers***,** 101063.

SERCK, C. S., FALEIDE, J. I., BRAATHEN, A., KJØLHAMAR, B. & ESCALONA, A. 2017a. Jurassic to early cretaceous basin configuration (s) in the Fingerdjupet Subbasin, SW Barents Sea. *Marine and Petroleum Geology,* 86**,** 874-891.

SERCK, C. S., FALEIDE, J. I., BRAATHEN, A., KJØLHAMAR, B., ESCALONA, A. J. M. & GEOLOGY, P. 2017b. Jurassic to early cretaceous basin configuration (s) in the Fingerdjupet Subbasin, SW Barents Sea. 86**,** 874-891.

SMELROR, M., PETROV, O., LARSSEN, G. & WERNER, C. 2009. *Atlas - Geological History of the Barents Sea*.

VERNIK, L. 2016. *Seismic petrophysics in quantitative interpretation*, Society of Exploration Geophysicists.

WALLES, F. 2004. A new method to help identify unconventional targets for exploration and development through integrative analysis of clastic rock property fields.

WORSLEY, D. 2008. The post-Caledonian development of Svalbard and the western Barents Sea. *Polar research,* 27**,** 298-317.

# Highlights for review

- Elastic parameter calculation points towards a two-fold caprock problem in the Hoop Fault complex
- High-resolution P-cable and conventional 3D seismic data with petrophysical well-data to investigate regional and local variations within caprock shales.
- Caprocks integrity assessment above ultra-shallow reservoirs
- Total Organic Content in shales can increase seal integrity in highly uplifted areas on the northern Barents Shelf.

**Declaration of interests**

☒The authors declare that they have no known competing financial interests or personal relationships that could have appeared to influence the work reported in this paper.

☐The authors declare the following financial interests/personal relationships which may be considered as potential competing interests: